

## 3,4-Methylenedioxypropylamphetamine (MDPV): in vitro mechanisms of hepatotoxicity under normothermic and hyperthermic conditions

Maria João Valente<sup>1</sup> · Ana Margarida Araújo<sup>1</sup> · Renata Silva<sup>1</sup> ·  
Maria de Lourdes Bastos<sup>1</sup> · Félix Carvalho<sup>1</sup> · Paula Guedes de Pinho<sup>1</sup> ·  
Márcia Carvalho<sup>1,2</sup>

Received: 28 September 2015 / Accepted: 18 November 2015 / Published online: 16 December 2015  
© Springer-Verlag Berlin Heidelberg 2015

**Abstract** Synthetic cathinones have emerged in recreational drug markets as legal alternatives for classical amphetamines. Though currently banned in several countries, 3,4-methylenedioxypropylamphetamine (MDPV) is one of the most commonly abused cathinone derivatives worldwide. We have recently reported the potential of MDPV to induce hepatocellular damage, but the underlying mechanisms responsible for such toxicity remain to be elucidated. Similar to amphetamines, a prominent toxic effect of acute intoxications by MDPV is hyperthermia. Therefore, the present in vitro study aimed to provide insights into cellular mechanisms involved in MDPV-induced hepatotoxicity and also evaluate the contribution of hyperthermia to the observed toxic effects. Primary cultures of rat hepatocytes were exposed to 0.2–1.6 mM MDPV for 48 h, at 37 or 40.5 °C, simulating the rise in body temperature that follows MDPV intake. Cell viability was measured through the MTT reduction and LDH leakage assays. Oxidative stress endpoints and cell death pathways were evaluated, namely the production of reactive oxygen and nitrogen species (ROS and RNS), intracellular levels of reduced (GSH) and oxidized (GSSG) glutathione, adenosine triphosphate (ATP) and free calcium (Ca<sup>2+</sup>), as well as the activities of caspases 3, 8 and 9, and nuclear morphological changes with Hoechst 33342/PI double staining. At 37 °C, MDPV induced a concentration-dependent loss of cell viability that was accompanied by GSH

depletion, as one of the first signs of toxicity, observed already at low concentrations of MDPV, with negligible changes on GSSG levels, followed by accumulation of ROS and RNS, depletion of ATP contents and increases in intracellular Ca<sup>2+</sup> concentrations. Additionally, activation of caspases 3, 8, and 9 and apoptotic nuclear morphological changes were found in primary rat hepatocytes exposed to MDPV, indicating that this cathinone derivative activates both intrinsic and extrinsic apoptotic death pathways. The cytotoxic potential of MDPV and all the studied endpoints were markedly aggravated under hyperthermic conditions (40.5 °C). In conclusion, these data suggest that MDPV toxicity in primary rat hepatocytes is mediated by oxidative stress, subsequent to GSH depletion and increased ROS and RNS accumulation, mitochondrial dysfunction, and impairment of Ca<sup>2+</sup> homeostasis. Furthermore, the rise in body temperature subsequent to MDPV abuse greatly exacerbates its hepatotoxic potential.

**Keywords** MDPV · Synthetic cathinones · Hepatotoxicity · Hyperthermia · Oxidative stress

### Abbreviations

MDPV	3,4-Methylenedioxypropylamphetamine
MDMA	3,4-Methylenedioxymethamphetamine
GSH	Reduced glutathione
GSSG	Oxidized glutathione
ROS	Reactive oxygen species
RNS	Reactive nitrogen species
ATP	Adenosine triphosphate

### Introduction

Synthetic cathinones are a broad group of novel psychostimulant substances, commonly known as ‘bath salts’,

✉ Maria João Valente  
mjoao.pcv@gmail.com

✉ Márcia Carvalho  
mcarv@ufp.edu.pt

<sup>1</sup> Laboratory of Toxicology, Faculty of Pharmacy, UCIBIO@REQUIMTE, Porto, Portugal

<sup>2</sup> FP-ENAS, CEBIMED, Fundação Ensino e Cultura Fernando Pessoa, Porto, Portugal

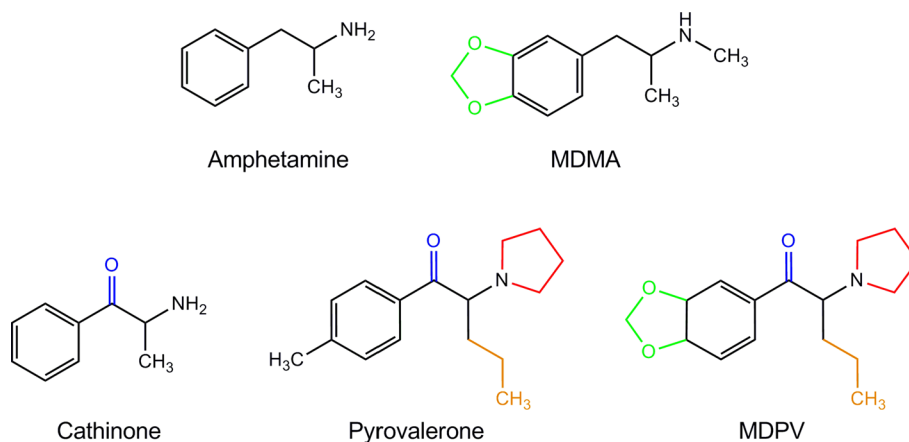
that originally appeared in the recreational drug markets as legal alternatives to classical illicit drugs, namely amphetamines and cocaine (for a comprehensive review on synthetic cathinones, please see Valente et al. 2014). Although recently regulated in several countries, cathinone derivatives are expanding into the illicit markets and, therefore, remain widely accessible in Internet Web sites and can also be purchased through street dealers (German et al. 2014; Johnson and Johnson 2014). This group of substances comprises structural derivatives of cathinone, a phenylalkylamine alkaloid naturally present in the khat plant (*Catha edulis*) (Valente et al. 2014). Cathinone is structurally related to amphetamine, differing only by the presence of a ketone group in the  $\beta$ -position of the alkylamine side chain (Fig. 1). For this reason, cathinone derivatives are often termed  $\beta$ -keto amphetamines. Based on the close chemical similarities, cathinone and cathinone-derived designer drugs share many of the pharmacological and behavioral characteristics commonly associated with the amphetamine psychostimulants, including increased locomotor activity (Aarde et al. 2013; Gatch et al. 2013; Jones et al. 2014; Lopez-Arnau et al. 2012), thermoregulatory disruption (Lopez-Arnau et al. 2015; Miller et al. 2013; Shortall et al. 2013) and the ability to produce discriminative stimulus effects (Fantegrossi et al. 2013; Gatch et al. 2013; Varner et al. 2013). From over seventy synthetic cathinone derivatives identified so far, 3,4-methylenedioxypropylpyrovalerone (MDPV) has received notoriety as a major component of ‘bath salts’ products (EMCDDA-Europol 2014; EMCDDA 2015; Zuba and Byrska 2013), and is one of the most commonly abused derivatives worldwide by virtue of its amphetamine- and cocaine-like effects (Johnson and Johnson 2014; Murray et al. 2012). Structurally, MDPV contains both a 3,4-methylenedioxy ring attached to the phenyl group similar to the well-known 3,4-methylenedioxymethamphetamine (MDMA, ‘ecstasy’), and a pyrrolidine ring in the side chain making it close to the psychostimulant pyrovalerone (Fig. 1). Not surprisingly,

MDPV induces MDMA-like subjective effects, including increased energy, mild empathogenic effects and sociability, and increased mental stimulation and sexual drive (Coppola and Mondola 2012a; Deluca et al. 2009; Kesha et al. 2013).

Information on the toxicological properties of these emerging drugs of abuse is limited, but several cases of ‘bath salts’-related intoxication and deaths have been reported over the last years (James et al. 2011; Murray et al. 2012; Wood et al. 2010). Most symptoms are consistent with sympathetic stimulation, including tachycardia, vasoconstriction, hypertension, hyperthermia, diaphoresis, mydriasis, respiratory distress, muscle tremor and spasms, muscle weakness, rhabdomyolysis, and seizures. Several other effects have been associated with intoxication by synthetic cathinones, including chest pain, myocardial infarction, stroke, disseminated intravascular coagulation, hepatic dysfunction, acute kidney injury, cerebral edema, coma, cardiovascular collapse, and death (Borek and Holstege 2012; Carhart-Harris et al. 2011; Coppola and Mondola 2012a, b; Fröhlich et al. 2011; Mugele et al. 2012).

The liver is a major target for many drugs of abuse, such as amphetamines and cocaine (Andreu et al. 1998; James et al. 2011; Kamijo et al. 2002; Kanel et al. 1990). Clinical evidence has shown that the liver is also a target of MDPV toxicity (Borek and Holstege 2012; Fröhlich et al. 2011; Murray et al. 2012). Based on the close chemical and pharmacological similarities shared by amphetamines and  $\beta$ -keto amphetamines, we hypothesized that cathinone derivatives would cause hepatotoxicity like their amphetamine counterparts. In line with this, our group has recently demonstrated the *in vitro* hepatotoxic potential of four of the most prevalent synthetic cathinones, namely methylone, MDPV, 4-methylethcathinone (4-MEC) and pentedrone (Araujo et al. 2015), with potencies similar to MDMA. However, specific mechanisms and pathways involved are completely unknown. Various factors may contribute to MDPV-induced liver toxicity, including hyperthermia.

**Fig. 1** Chemical structures of amphetamine, MDMA, cathinone, pyrovalerone and MDPV. *MDMA* 3,4-methylenedioxymethamphetamine, *MDPV* 3,4-methylenedioxypropylpyrovalerone (color figure online)



The impairment of thermoregulation elicited by MDPV has also been reported, with significant increases in human body temperature up to values ranging between 39.5 and 41.7 °C (Borek and Holstege 2012; Fröhlich et al. 2011; Kesha et al. 2013; Mugele et al. 2012; Murray et al. 2012). It must be stressed that hyperthermia *per se* is a pro-oxidant aggressive condition (Skibba et al. 1991; Wills et al. 1976), which may render liver cells more vulnerable to oxidants. Accordingly, our group has previously shown that hyperthermia acts synergistically with MDMA-induced toxicity toward freshly isolated mouse hepatocytes (Carvalho et al. 2001) and primary cultured rat hepatocytes (Pontes et al. 2008), but it remains to be investigated whether hyperthermia also exacerbates MDPV toxic responses *in vitro*. Therefore, the goal of the present study was to provide insights into the mechanisms involved in the toxicity elicited by MDPV in primary cultures of rat hepatocytes under normothermic and hyperthermic conditions (37 and 40.5 °C, respectively). The specific objectives of this study were to (1) evaluate the cytotoxic effect of MDPV in primary rat hepatocytes; (2) elucidate the biochemical mechanisms underlying the cellular injury, namely the generation of ROS and RNS, the interference of MDPV in the homeostasis of glutathione and calcium, and with mitochondrial function; (3) characterize the nature of cell death in MDPV-exposed rat hepatocytes; and (4) investigate the role of hyperthermia in MDPV hepatotoxicity.

## Materials and methods

### Chemicals

Hank's balanced salt solution (HBSS), heat-inactivated fetal bovine serum (FBS), antibiotic mixture of penicillin/streptomycin (10,000 U/mL/10,000 µg/mL) and fungizone (250 µg/mL) were obtained from GIBCO Invitrogen (Barcelona, Spain). Collagenase from *Clostridium histolyticum* Type IA, bovine serum albumin (BSA), 4-(2-hydroxyethyl)-piperazine-1-ethanesulfonic acid (HEPES), ethylene glycol-bis-(2-aminoethylether)-N,N,N',N'-tetraacetic acid (EGTA), dithiothreitol (DTT), ethylenediaminetetraacetic acid (EDTA), Williams' E Medium, dexamethasone, gentamicin sulfate salt, insulin solution from bovine pancreas (10 mg/mL), thiazolyl blue tetrazolium bromide (MTT), sodium pyruvate, β-nicotinamide adenine dinucleotide reduced disodium salt hydrate (β-NADH), 2',7'-dichlorodihydrofluorescein (DCFH) and 2',7'-dichlorodihydrofluorescein diacetate (DCFH-DA), L-glutathione reduced (GSH) and L-glutathione oxidized disodium salt (GSSG), β-nicotinamide adenine dinucleotide 2'-phosphate reduced tetrasodium salt hydrate (β-NADPH), 5,5'-dithiobis(2-nitrobenzoic

acid) (DTNB), adenosine triphosphate (ATP), luciferase from *Photinus pyralis* (firefly) and D-luciferin sodium salt, N-acetyl-Asp-Glu-Val-Asp-*p*-nitroanilide (Ac-DEVD-pNA, caspase 3 substrate), N-acetyl-Ile-Glu-Thr-Asp-*p*-nitroanilide (Ac-IETD-pNA, caspase 8 substrate), and N-acetyl-Leu-Glu-His-Asp-*p*-nitroanilide (Ac-LEHD-pNA, caspase 9 substrate) were purchased from Sigma-Aldrich (St. Louis, MO). Fluo-3 AM, FluoroPure™ grade was obtained from Molecular Probes (Eugene, OR, USA). All other chemicals, of analytical grade, were purchased from Merck (Darmstadt, Germany). MDPV hydrochloride was purchased online from the Sensearomatic website (<http://sensearomatic.net>, currently unavailable), during March 2013. The salt was fully characterized by mass spectrometry, Nuclear Magnetic Resonance (NMR), and elemental analysis, and purity was greater than 98 %.

### Isolation and primary culture of rat hepatocytes

Rat hepatocytes were isolated from male Wistar Han rats (200–250 g) purchased from Charles-River Laboratories (Barcelona, Spain). All experiments were approved by the local ethics committee for the welfare of experimental animals and performed in accordance with national legislation. Surgical procedures were conducted under anesthesia by inhalation of isoflurane, in an isolated system, and carried out between 10.00 and 11.00 a.m. Cells were isolated through a collagenase perfusion, as previously described by our group (Pontes et al. 2008). Briefly, a cannula was inserted in the hepatic portal vein, and the liver was perfused initially with Hank's washing buffer containing BSA and the chelating agent EGTA, followed by a solution of collagenase supplemented by its co-factor calcium. The liver capsule was then gently disrupted in order to release isolated liver cells into a Krebs–Henseleit buffer. The cell suspension was subsequently purified through three cycles of low-speed centrifugations (300 rpm, for 2 min). The final suspension was then incubated with penicillin/streptomycin (500 U/mL/500 µg/mL), at 4 °C, for 30 min. Cell viability was estimated by the trypan blue exclusion test and was always higher than 80 %. A suspension of 500,000 viable cells/mL was cultured in 6- or 96-well plates at approximately 100,000 cells/cm<sup>2</sup>, in William's E medium, supplemented with 10 % FBS, 100 U/mL/100 µg/mL penicillin/streptomycin, 5 µg/mL insulin, 50 µM dexamethasone, 100 µg/mL gentamicin and 2.5 µg/mL fungizone, and incubated overnight at 37 °C, with 5 % CO<sub>2</sub>, to allow cell adhesion.

### Cell viability assays

Hepatocytes were seeded in 96-well plates and exposed to MDPV at a concentration range that includes low-effect

to worst-case approach concentrations (0.2–1.6 mM) in serum-free medium, under normothermic (37 °C) and hyperthermic (40.5 °C) conditions. Cell viability was evaluated after 48 h through the MTT reduction assay and confirmed by the LDH leakage assay, as previously described (Araujo et al. 2015; Barbosa et al. 2014), with minor modifications. For the MTT reduction assay, cells were incubated with a solution of 0.5 mg/mL MTT for 80 min, and the formazan crystals formed through mitochondrial succinate dehydrogenase were dissolved in DMSO and detected at 550 nm in a 96-well plate reader (PowerWaveX; Bio-Tek, Winooski, VT, USA). For measurement of the amount of LDH released into the culture medium, the plates were centrifuged for 10 min at 250g, and 50 µL of the incubation medium (dilutions prepared in phosphate buffer: 50 mM KH<sub>2</sub>PO<sub>4</sub>, pH 7.4) were collected from each well in duplicates into new 96-well plates, to which 200 µL of a 0.21 mM β-NADH solution were added. The kinetic oxidation of β-NADH into β-NAD<sup>+</sup> after adding 25 µL of 22.7 mM sodium pyruvate was monitored at 340 nm in a 96-well absorbance plate reader. Data were normalized to a no-effect (no treatment) and a maximum-effect (lysed with 1 % Triton X-100) controls.

### Characterization of hepatotoxicity mechanisms triggered by MDPV

#### *Measurement of intracellular GSH and GSSG levels*

Total glutathione (tGSH) and oxidized glutathione (GSSG) contents were determined through the DTNB-GSSG reductase recycling assay (Carvalho et al. 2004). For this purpose, hepatocytes were seeded in 6-well plates and exposed to MDPV, at 37 °C or 40.5 °C. After a 48 h incubation period, cells were rinsed with HBSS without calcium and magnesium, scrapped and precipitated with 5 % perchloric acid for 20 min, at 4 °C. Suspensions were centrifuged at 6000g, for 5 min, at 4 °C, and the supernatant was then neutralized with 0.76 M KHCO<sub>3</sub>, on ice. The samples were spun at 13,000 rpm, and 100 µL of the supernatants were added to a 96-well plate, followed by 65 µL of a freshly prepared reagent solution of 71.5 mM phosphate buffer with 0.63 mM EDTA containing 0.7 mM NADPH and 4 mM DTNB. Samples were incubated for 15 min at 30 °C in a thermomax 96-well plate reader, and 40 µL of 10 U/mL glutathione reductase was then rapidly added to all samples. The consequent formation of 5-thio-2-nitrobenzoic acid (TNB) was followed for 2 min at 415 nm and compared with a GSH standard curve prepared in 5 % HClO<sub>4</sub>. For GSSG quantification, precipitated samples were incubated with 2-vinylpyridine for 1 h, at 4 °C, with continuous agitation, in order to derivatize GSH. GSSG was then quantified as described for tGSH. All data were normalized to total

protein content of each sample, measured by the Lowry method, using standard stock solutions of BSA. GSH levels were calculated by subtracting GSSG content from tGSH values as follows:  $GSH = tGSH - (2 \times GSSG)$ .

#### *Measurement of intracellular reactive oxygen and nitrogen species*

Intracellular generation of reactive oxygen (ROS) and nitrogen (RNS) species was monitored via DCFH-DA fluorescence assay as previously described (da Silva et al. 2014). DCFH-DA is a cell-permeable fluorogenic probe that readily diffuses into the cells, where it is deacetylated by cellular esterases, and the resultant non-fluorescent DCFH is further oxidized by ROS and RNS to the highly fluorescent 2',7'-dichlorofluorescein (DCF). For this assay, after overnight cell adhesion in 96-well plates, hepatocytes were pre-incubated with 10 µM DCFH-DA, at 37 °C, protected from light. After 30 min, cells were rinsed with HBSS without calcium and magnesium and incubated with 0.2–1.6 mM MDPV for 48 h, at 37 or 40.5 °C. The fluorescence was then recorded on a microplate reader (Synergy HTX Multi-Mode Reader; Bio-Tek, Winooski, VT, USA), set to 485 nm excitation and 530 nm emission. Results were normalized to negative controls (no treatment) and calculated as fold increase over control. No interference with the probe was noted at any tested concentration of MDPV, as determined by incubation for 48 h with DCFH in the absence of cells (data not shown).

#### *Measurement of intracellular ATP levels*

The ATP bioluminescence assay is based on the emission of light from the reaction of ATP and luciferin, catalyzed by luciferase and was performed as previously described (Valente et al. 2012). After exposure to MDPV, cells were rinsed and treated as described above for tGSH measurement. After neutralization, samples were spun, and 100 µL of the supernatants were added to 96-well opaque plates with 100 µL of luciferin–luciferase assay solution [final concentrations: 0.15 mM luciferin, 30,000 light units luciferase, 50 mM glycine, 10 mM MgSO<sub>4</sub>, 1 mM Tris, 0.55 mM EDTA, 1 % BSA (pH 7.6)]. ATP calibration curve was obtained with standard stock solutions of ATP prepared in 5 % HClO<sub>4</sub>. Results were normalized to total protein, measured by the Lowry method.

#### *Quantification of intracellular free calcium (Ca<sup>2+</sup>) levels by flow cytometry*

Fluo3-AM is a sensitive fluorochrome that is enzymatically hydrolyzed by cellular esterases to give Fluo3, which exhibits an increase in fluorescence upon binding with

calcium. For this assay, cells from six-well plates exposed to 0.2–1.6 mM MDPV for 48 h were collected after trypsinization with 0.05 % trypsin/EDTA, centrifuged (250g, 5 min, 4 °C), and rinsed with HBSS without calcium and magnesium. After further centrifugation, the supernatant was discarded and samples were incubated for 30 min, with continuous agitation, at 37 °C, with 50 µL of a 10 µM Fluo3-AM solution prepared in serum-free Williams' E Medium without phenol red. Following incubation, the cells were washed and resuspended with HBSS with calcium and magnesium and kept on ice until further analysis. Samples were analyzed in a BD Accuri™ C6 flow cytometer (BD Biosciences, CA, USA), with the FCS Express™ analysis software. The green fluorescence of Fluo3 was detected through a 533/30 nm filter (FL1 detector). The DNA of non-viable cells was stained with 5 µg/mL propidium iodide (PI), which has a maximum fluorescence emission at 617 nm, and the green fluorescence from PI positive cells was excluded from the analysis. At least 20,000 viable cells were analyzed per sample. There was no contribution of autofluorescence, as determined by the analysis of treated cells in the absence of Fluo3-AM (data not shown). Data were normalized to controls without treatment.

### Characterization of death pathways triggered by MDPV

#### *Measurement of caspase 3, 8 and 9 activity*

The activities of caspase 3, 8 and 9 were determined in cytoplasmatic fractions of hepatocytes after exposure to 0.2–1.6 mM MDPV for 48 h, as previously described (Capela et al. 2007), with adaptations. This assay was based on the hydrolysis of the peptide substrates for each caspase, namely Ac-DEVD-pNA, Ac-IETD-pNA and Ac-LEHD-pNA, for caspase 3, 8 and 9, respectively. This reaction results in the release of the p-nitroaniline moiety, with peak absorbance at 405 nm. For each condition, three wells of a 6-well plate were rinsed with HBSS without calcium and magnesium, and pellets were collected into new tubes with 225 µL of lysis buffer [final concentrations: 50 mM HEPES, 1 mM DTT, 0.1 mM EDTA, 0.1 % CHAPS (pH 7.4)]. Samples were incubated for 5 min on ice, centrifuged (16,000g, 10 min, 4 °C), and the cell lysate transferred into new tubes. Two hundred microliters of assay buffer [final concentrations: 100 mM NaCl, 50 mM HEPES, 10 mM DTT, 1 mM EDTA, 10 % glycerol, 0.1 % CHAPS (pH 7.5)] were added to 50 µL of lysate in 96-well plates, followed by 5 µL of colorimetric substrate (16 µM Ac-DEVD-pNA, 200 µM Ac-IETD-pNA or 200 µM Ac-LEHD-pNA). After 24 h at 37 °C, absorbance was determined at 405 nm in a 96-well absorbance plate reader. Protein content in cell lysate was measured

using the Bio-Rad RC DC protein assay kit (Hercules, CA, USA), with BSA as the standard.

#### *Hoechst 33342/propidium iodide fluorescent staining*

Apoptotic hepatocytes were identified based on chromatin morphology, as previously described (Valente et al. 2012), using Hoechst 33342, a cell-permeant nuclear counterstain that emits blue fluorescence when bound to DNA, and PI, a membrane impermeant nuclear dye that emits red fluorescence only in dead cells. Briefly, primary rat hepatocytes were seeded into six-well plates and exposed to MDPV (0.2–1.6 mM) for 48 h, at 37 or 40.5 °C. After washing with HBSS without calcium and magnesium, cells were incubated with 50 µM PI for 15 min, rinsed again, and fixed with a 4 % solution of p-formaldehyde for 20 min. After washing, cells were incubated with a 5 µg/mL Hoechst 33342 solution for 5 min and observed under a fluorescent microscope.

### Statistical analysis

Data were obtained from at least five independent experiments, performed in duplicate or triplicate, and are presented as mean ± standard error of the mean (SEM). Statistical analysis was performed using the GraphPad Prism 6 (version 6.01) for Windows. Multiple comparisons within the two variables (concentration and temperature) were performed through one-way ANOVA analysis, followed by Fisher's LSD post hoc test. Significance was accepted for  $p < 0.05$ .

## Results

### MDPV induces cell death in a concentration-dependent manner, exacerbated in hyperthermic conditions

The data presented in Fig. 2 show a concentration-dependent increase in cytotoxicity, as determined by the MTT reduction assay, in primary rat hepatocytes exposed to MDPV at 37 °C. This effect was significant ( $p < 0.01$  vs. control), even at the lowest concentration tested (0.2 mM). Since MDPV is a ketone, and thus, a possible redox electron donor that may interfere with redox-based tests like the MTT assay (den Hollander et al. 2014), we additionally performed the interference-free and unbiased LDH leakage assay, under the same experimental conditions, and the obtained results are shown in Fig. 3. Data from this assay corroborate the results from the MTT test, showing cell death in identical magnitude and significance, which suggests that there is no substantial reduction of the tetrazolium dye by MDPV under our in vitro conditions.

**Fig. 2** Effects of MDPV on MTT reduction in primary cultured rat hepatocytes. Hepatocytes were exposed for 48 h, at 37 or 40.5 °C, to 0.2–1.6 mM MDPV. Results are presented as mean  $\pm$  SEM from at least five independent experiments, performed in triplicate. \*\* $p < 0.01$ , \*\*\*\* $p < 0.0001$  versus control. # $p < 0.05$ , #### $p < 0.0001$  versus normothermia

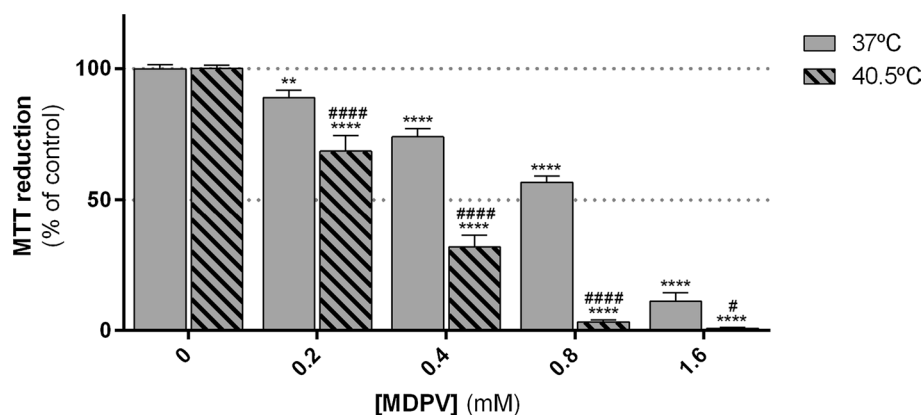
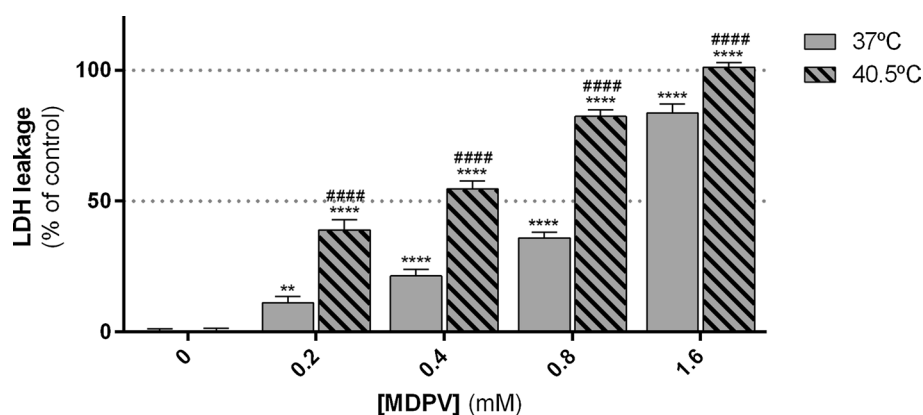


**Fig. 3** Effects of MDPV on LDH leakage in primary cultured rat hepatocytes. Hepatocytes were exposed for 48 h, at 37 or 40.5 °C, to 0.2–1.6 mM MDPV. Results are presented as mean  $\pm$  SEM from six independent experiments, performed in triplicate. \*\* $p < 0.01$ , \*\*\*\* $p < 0.0001$  versus control. ##### $p < 0.0001$  versus normothermia



Noteworthy, a rise in incubation temperature from 37 to 40.5 °C greatly exacerbated cell death induced by MDPV, for all concentration range ( $p < 0.0001$  vs. normothermia). For instance, as observed in the MTT assay, cell death induced by 0.2 mM MDPV increased from  $11.1 \pm 2.9$  % in normothermic conditions up to  $31.4 \pm 5.9$  % in hyperthermic conditions.

### MDPV triggers a marked GSH depletion and ROS and RNS formation in primary rat hepatocytes, exacerbated in hyperthermic conditions

Since oxidative stress is a well-known mechanism involved in the hepatotoxicity of non-keto amphetamines (Carvalho et al. 2012), we started to investigate whether this mechanism is also shared by MDPV. Glutathione provides a major cell antioxidant defense against reactive species formation and ensuing oxidative damage. Therefore, the intracellular content of GSH and GSSG was measured after exposure of primary rat hepatocytes to MDPV (0.2–1.6 mM), at 37 and 40.5 °C. As depicted in Fig. 4a, at 37 °C, MDPV caused a significant concentration-dependent decline in GSH levels, with a decrease from  $39.1 \pm 3.2$  nmol/mg of protein in control cells to  $15.4 \pm 2.9$  nmol/mg of protein in cells treated with 1.6 mM MDPV. GSH depletion was clearly more

accentuated under hyperthermic conditions. In fact, the highest concentration studied (1.6 mM) caused an almost complete depletion of GSH levels ( $0.4 \pm 0.1$  nmol/mg of protein) at 40.5 °C ( $p < 0.0001$  vs. control and normothermia). An important finding was that, under normothermic conditions, the GSH depletion induced by MDPV was not accompanied by glutathione oxidation (Fig. 4b). However, it is noteworthy that hyperthermia, by itself, elicited a significant decline in basal GSH levels of control cells of approximately 36 % ( $p < 0.0001$ ), as well as an increase of nearly 100 % in GSSG levels ( $p < 0.05$ ).

The involvement of oxidative stress in MDPV-induced toxicity was further assessed through the measurement of ROS and RNS generation at the same conditions. The levels of reactive species following 48 h exposure with MDPV at normothermic and hyperthermic conditions are shown in the Fig. 5. At 37 °C, MDPV increased the formation of reactive species after exposure to the highest concentration studied (1.6 mM), with a  $1.50 \pm 0.04$ -fold increase over control cells ( $p < 0.0001$  vs. control). At 40.5 °C, the levels of ROS and RNS were prominently increased in a concentration-dependent manner following incubation with MDPV, with a  $1.14 \pm 0.03$ ,  $1.29 \pm 0.03$  and  $1.65 \pm 0.06$ -fold increase in cells treated with 0.4, 0.8 and 1.6 mM MDPV, respectively.

**Fig. 4** Effects of MDPV on **a** GSH and **b** GSSG levels in primary cultured rat hepatocytes. Hepatocytes were exposed for 48 h, at 37 or 40.5 °C, to 0.2–1.6 mM MDPV. Results are presented as mean  $\pm$  SEM from at least five independent experiments, performed in triplicate. Please note that different scales on the y-axis are used in **a** and **b**. \* $p < 0.05$ , \*\*\* $p < 0.001$ , \*\*\*\* $p < 0.0001$  versus control. # $p < 0.05$ , #### $p < 0.0001$  versus normothermia

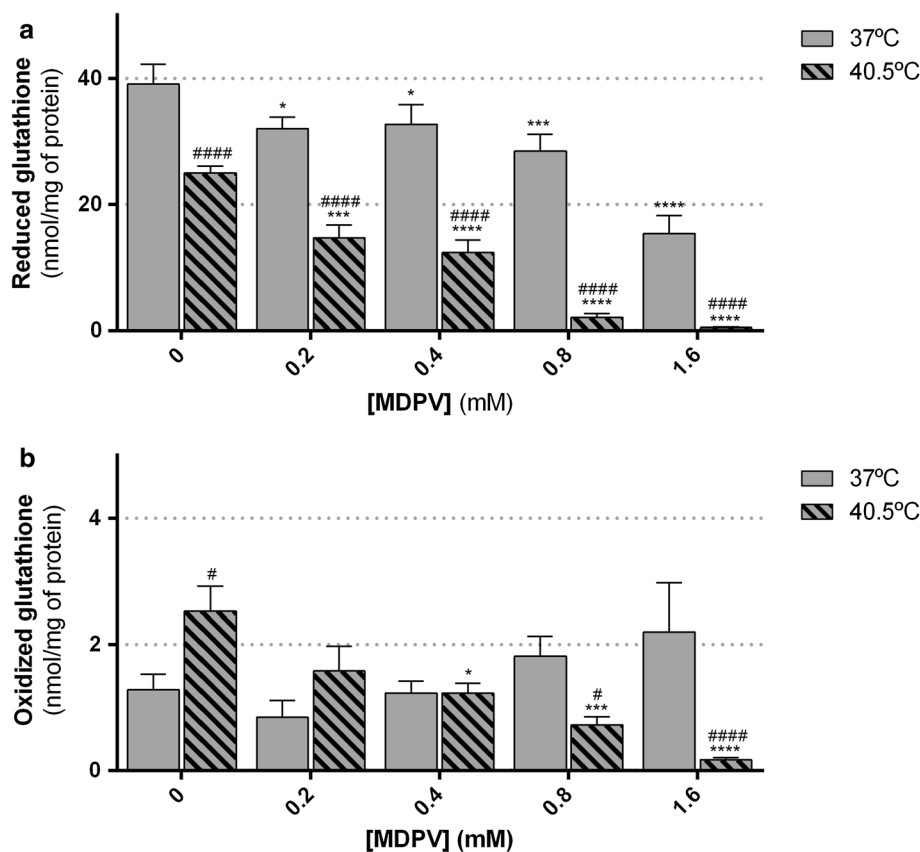
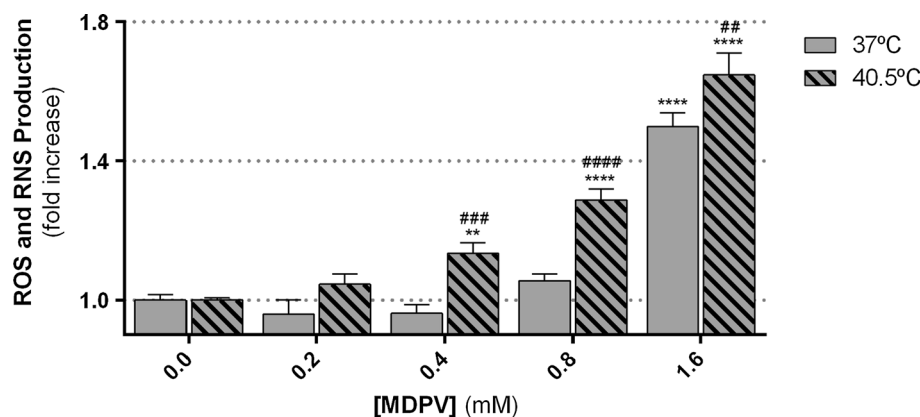


**Fig. 5** Effects of MDPV on ROS and RNS production in primary cultured rat hepatocytes. Hepatocytes were exposed for 48 h, at 37 or 40.5 °C, to 0.2–1.6 mM MDPV. Results are presented as mean  $\pm$  SEM from six independent experiments, performed in triplicate. \*\* $p < 0.01$ , \*\*\*\* $p < 0.0001$  versus control. ## $p < 0.01$ , ### $p < 0.001$ , #### $p < 0.0001$  versus normothermia



### MDPV hampers the hepatocellular energetic status and $\text{Ca}^{2+}$ homeostasis, especially at high concentrations and in hyperthermic conditions

To better understand the potential mechanisms involved in MDPV-induced toxicity in primary rat hepatocytes, we investigated whether mitochondrial bioenergetic function or calcium homeostasis are affected. Figure 6 depicts the intracellular levels of ATP in MDPV-treated cells at both incubation temperatures herein studied (37 and 40.5 °C). At 37 °C, it was observed a pronounced decline (from  $23.6 \pm 4.2$  to  $8.3 \pm 1.6$  nmol/mg of protein) in intracellular

ATP levels in cells exposed to 1.6 mM MDPV ( $p < 0.001$  vs. control), with no significant changes detected at lower concentrations. The increase in incubation temperature to 40.5 °C prompted an abrupt energy depletion in hepatocytes treated with 0.8 mM and 1.6 mM MDPV (from  $22.7 \pm 1.9$  in control cells to  $1.8 \pm 0.3$  and  $0.3 \pm 0.1$  nmol/mg, respectively), and to a less extent with 0.4 mM MDPV. Moreover, as shown in Fig. 7, MDPV at these two highest concentrations also affects the intracellular  $\text{Ca}^{2+}$  homeostasis, whereas no significant changes were noticed at lower concentrations. No statistically significant differences were detected between normo- and hyperthermic conditions.

**Fig. 6** Effects of MDPV on ATP levels in primary cultured rat hepatocytes. Hepatocytes were exposed for 48 h, at 37 or 40.5 °C, to 0.2–1.6 mM MDPV. Results are presented as mean  $\pm$  SEM from at least five independent experiments, performed in duplicate. \*\*\* $p$  < 0.001, \*\*\*\* $p$  < 0.0001 versus control. # $p$  < 0.05, #### $p$  < 0.0001 versus normothermia

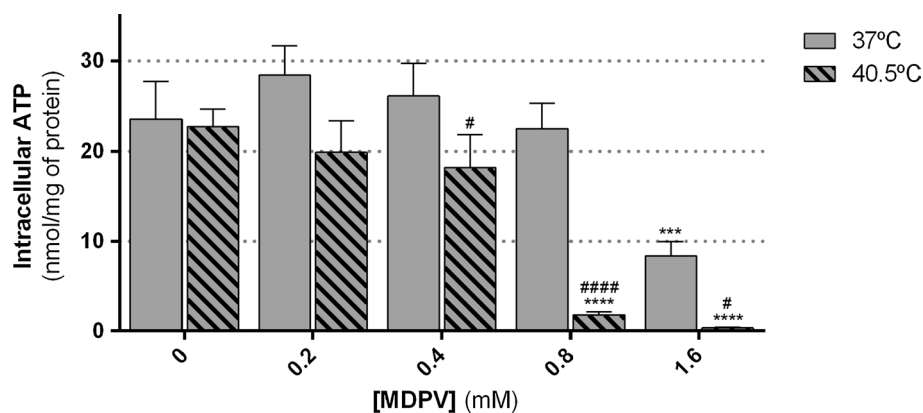
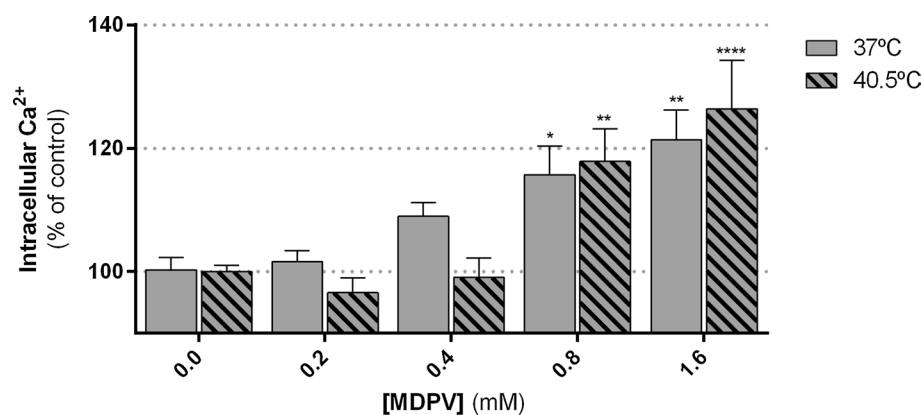


**Fig. 7** Effects of MDPV on intracellular  $\text{Ca}^{2+}$  levels in primary cultured rat hepatocytes. Hepatocytes were exposed for 48 h, at 37 or 40.5 °C, to 0.2–1.6 mM MDPV. Results are presented as mean  $\pm$  SEM from at least five independent experiments, performed in duplicate. \* $p$  < 0.05, \*\* $p$  < 0.01, \*\*\* $p$  < 0.001 versus control



### MDPV induces primarily apoptotic cell death in normothermia, but shifts to necrosis under hyperthermic conditions

To determine whether MDPV-induced hepatotoxicity involves the initiation of apoptotic cell death mechanisms, two different methodological approaches were followed: (1) fluorescence microscopy analysis after staining with Hoechst 33342/PI and (2) measurement of caspase 3, 8 and 9 activity. Nuclear morphological changes of MDPV-treated primary rat hepatocytes were examined using Hoechst 33342, a membrane permeable blue dye for DNA labeling, and PI, a fluorescent red dye that intercalates into double-stranded nucleic acid of late apoptotic or necrotic cells. Figure 8 shows representative Hoechst 33342/PI fluorescence photomicrographs of cultured cells treated with and without MDPV at two different incubation temperatures. In control cells, at 37 °C, nuclei appeared with regular contours and were round and large in size, whereas, at 40.5 °C, it was possible to identify early apoptotic events (pyknotic nuclei formation without PI label, green arrows). In MDPV-treated cells, under normothermic conditions, the pyknotic nuclei were visible even at the lowest MDPV concentration tested, as well as late apoptotic cells (red condensed nuclei). On the other hand, necrotic cells (red large nuclei) were only observable in 0.8

and 1.6 mM MDPV-exposed cells. In contrast, a rise in incubation temperature to 40.5 °C clearly favoured necrosis in hepatocytes treated with MDPV, as red large nuclei are seen under exposure to concentrations as low as 0.2 mM.

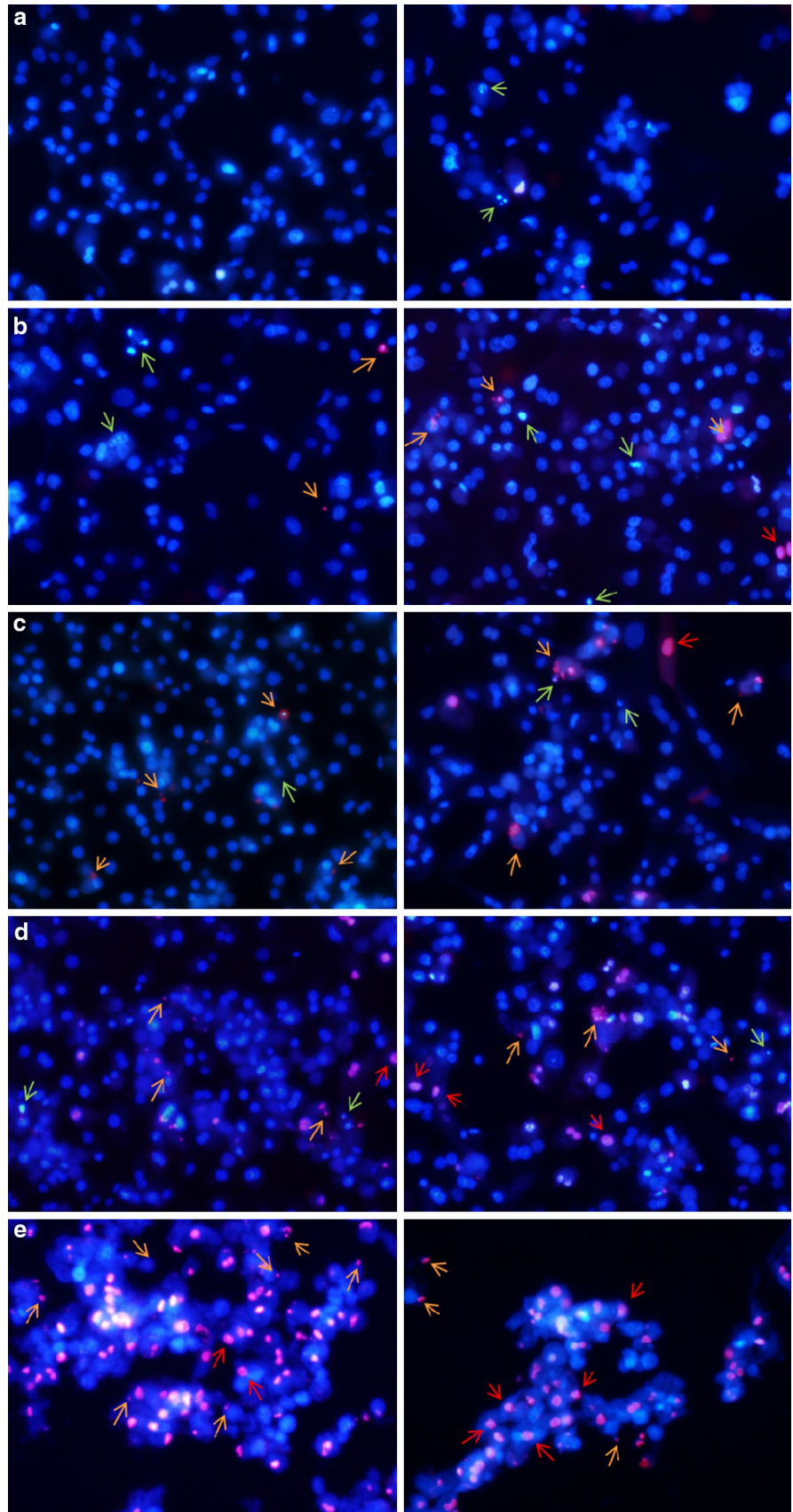
Since caspase activation is one of the main events leading to apoptosis, we additionally confirmed apoptotic cell death by evaluating the activation of caspases 8 (extrinsic pathway), 9 (intrinsic pathway), and 3 (effector caspase) at 37 and 40.5 °C. As can be seen in Fig. 9, at 37 °C, 1.6 mM MDPV significantly increased caspase 3, 8 and 9 activities in primary rat hepatocytes about 118, 55 and 54 % over control values, respectively ( $p$  < 0.0001 vs. control). Noteworthy, the increase in incubation temperature to 40.5 °C triggers caspase activation at lower concentrations. Under hyperthermia, a peak in caspase activation was achieved at 0.8 mM MDPV, with increases up to 156, 64 and 50 % over control values ( $p$  < 0.0001 vs. control), and further reduced at 1.6 mM MDPV to values near to controls for caspase 8 and 9 ( $p$  > 0.05 vs. control,  $p$  < 0.001 vs. normothermia), respectively.

### Discussion

MDPV structure is closely related to amphetamines that are known to be hepatotoxic in humans (Carvalho et al. 2012).



**Fig. 8** Representative fluorescence microscopy images of Hoechst 33342/PI staining. Hepatocytes were exposed for 48 h, at (left) 37 or (right) 40.5 °C, to **a** 0, **b** 0.2, **c** 0.4, **d** 0.8 or **e** 1.6 mM MDPV. *Green arrows* indicate early apoptotic cells, *orange arrows* indicate late apoptotic cells and *red arrows* indicate necrotic cells. Original magnification,  $\times 200$  (color figure online)



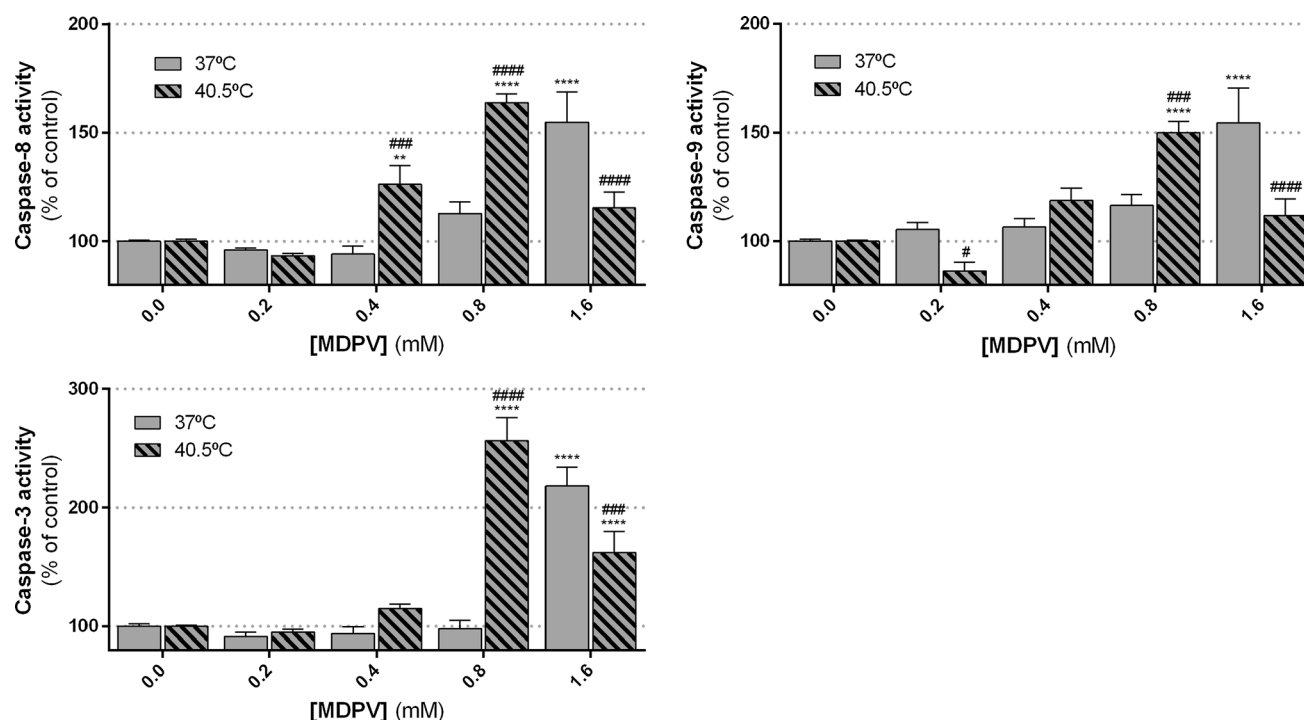


**Fig. 9** Effects of MDPV on the activities of caspases 3, 8 and 9 in primary cultured rat hepatocytes. Hepatocytes were exposed for 48 h, at 37 or 40.5 °C, to 0.2–1.6 mM MDPV. Results are presented as

mean  $\pm$  SEM from at least five independent experiments, performed in duplicate. \*\* $p$  < 0.01, \*\*\*\* $p$  < 0.0001 versus control. # $p$  < 0.05, ### $p$  < 0.001, #### $p$  < 0.0001 versus normothermia

Therefore, toxicological studies of cathinone designer drugs toward liver cells are of particular interest. In this study, we first tested and confirmed the ability of the synthetic cathinone MDPV to induce cytotoxicity in primary rat hepatocytes and contributed to the elucidation of the mechanisms involved in MDPV-induced hepatocellular injury at normothermia and hyperthermia. We showed that MDPV-induced cell death in a concentration- and temperature-dependent manner, through two different cytotoxicity tests, namely by inhibiting the reduction of MTT and promoting LDH leakage (Figs. 2, 3, respectively). These findings are consistent with our previous study showing the hepatotoxic potential of four of the most widely abused cathinone derivatives, including MDPV (Araujo et al. 2015).

Several mechanisms induced by drugs of abuse may lead to liver damage. Among them, oxidative stress is thought to play a major role in the hepatocellular damage consequent to the abuse of amphetamines (Beitia et al. 2000; Carvalho et al. 2010). Due to structural similarities to their non-keto congeners, we hypothesize that synthetic cathinones may undergo similar mechanisms of toxicity. In fact, our results suggest that MDPV and/or its intermediate metabolites, similarly to MDMA (Cerretani et al. 2011), cause oxidative stress in the liver, as evidenced by substantial depletion in the intracellular levels of GSH (Fig. 4a), which is

an endogenous antioxidant known to play a crucial role in cell survival, and increased formation of ROS and NOS (Fig. 5). Importantly, we found that MDPV-induced GSH depletion was not accompanied by an increase in GSSG levels. This result might be explained by ATP-dependent export of the formed GSSG into the extracellular space (Leier et al. 1996). However, in this experiment, GSH depletion seems to be primarily related to the formation of conjugates of MDPV with GSH, rather than a direct effect of reactive species, since the rise in ROS and RNS production was only observed in cells exposed to MDPV at high concentrations, where a severe GSH depletion in the cytosolic GSH pool had already occurred. In accordance, metabolic activation to a reactive metabolite capable of conjugating with GSH has been recently demonstrated for MDPV in vitro using human liver microsomes (Meyer et al. 2014; Strano-Rossi et al. 2010), and in vivo in rats and humans (Meyer et al. 2010) and, most certainly, occurs in our in vitro model. Therefore, MDPV metabolism and the ensuing depletion of intracellular GSH levels lowers the capacity of the cells to scavenge reactive species, enhancing oxidative stress, disturb cellular function and, ultimately, may lead to cell death.

Moreover, it must be highlighted that hepatic metabolism of amphetamines that contain a 3,4-methylenedioxy ring is an important source of ROS and other chemically

reactive compounds (Carvalho et al. 2010, 2012). This methylenedioxy group is also present in MDPV but, presently, it is not clear if any MDPV metabolites formed in cells are capable to undergo oxidation into reactive orthoquinones that enter redox cycling with subsequent production of ROS and RNS, as has been thoroughly described for MDMA (Carvalho et al. 2010). Therefore, it is still unknown whether the generation of reactive species in hepatocytes exposed to MDPV depends either on disturbance of the mitochondrial respiratory chain (well-known as the major cellular source of ROS generation) or MDPV metabolism, or even a combination of both.

There is a complex cross-talk between oxidative stress,  $\text{Ca}^{2+}$  homeostasis and mitochondrial function. As the main organelles responsible for ATP production, mitochondria are the core of cell energy supply and participate actively in the sequestration of free  $\text{Ca}^{2+}$  (Brookes et al. 2004). Our results showed that MDPV, at a high concentration (1.6 mM), triggered a drastic ATP depletion (Fig. 6). The lack of ATP might lead to a less efficient calcium control and mitochondrial electron chain regulation, as can be seen with the increase in intracellular  $\text{Ca}^{2+}$  content in primary rat hepatocytes treated with 1.6 mM MDPV for 48 h at 37 °C (Fig. 7), thus indicating that the mitochondrial function and calcium homeostasis are severely impaired by MDPV at high concentrations. This decreases in ATP levels occurred at a concentration where GSH depletion was almost complete, with overproduction of ROS and RNS, suggesting that oxidative stress may be involved in the disturbance of mitochondrial functions. On the other hand, it is possible that MDPV and/or its metabolites may inhibit the mitochondrial function by directly interacting with mitochondrial proteins. Further studies are necessary to determine the mechanisms of mitochondrial impairment induced by MDPV.

As center of cell death control, mitochondria undergo extensive membrane integrity and permeability changes prior to cell death itself (Tait and Green 2010). The mitochondrial permeability transition pore (MPTP), a large nonspecific conductance channel assembled from proteins in the inner and outer mitochondrial membranes, appears to play a key role in triggering of an intrinsic apoptotic pathway, and  $\text{Ca}^{2+}$  is also in control of the process of MPTP opening (Brookes et al. 2004; Halestrap 2009). In fact, Baumgartner et al. (2009) showed that the elevation of mitochondrial  $\text{Ca}^{2+}$  is the decisive factor in determining whether cells undergo oxidative stress-induced apoptosis. When there is an overload of  $\text{Ca}^{2+}$  in the mitochondrial matrix, the MPTP opens and allows free passage of ions and solutes under 1500 Da across the mitochondrial inner membrane. This effect has two outcomes: entering of protons that lead to uncoupling of the oxidative phosphorylation, and consequent impairment of ATP synthesis

(Halestrap 2006, 2009); and swelling of the mitochondria matrix, with subsequent rupture of the outer membrane, and nonspecific release of pro-apoptotic proteins into the cytosol, including cytochrome *c* (Tait and Green 2010). Alternatively, permeabilization of the outer mitochondrial membrane can be achieved by pore formation by pro-apoptotic Bcl-2 family proteins (Bax and Bak) (Tsujimoto 2003). Once in the cytosol, cytochrome *c* triggers a complex signaling cascade that ultimately ends in cell death through apoptosis, with activation of caspase 9, which further cleaves and activates the executioner caspases 3 and 7 that, in turn, cleave intracellular substrates, causing the morphological and biochemical changes observed in the process of apoptosis. These caspases may also enter the mitochondrial intermembrane space, disrupting the respiratory chain, consequently leading to a decline in ATP synthesis and increase in ROS production, which further amplifies apoptosis (McIlwain et al. 2013; Tait and Green 2010). Besides this intrinsic pathway, xenobiotics may also induce mitochondria-independent apoptotic pathways. This extrinsic process is initiated by the binding of ligands to death receptors located in the cell membrane, leading to the activation of caspase 8, which directly initiates apoptosis by activating the executioner caspases, or indirectly activating the intrinsic apoptotic pathway (McIlwain et al. 2013).

In the present study, it was demonstrated that MDPV-treated primary rat hepatocytes stained with Hoechst 33342/PI, in the absence of heat stress (at 37 °C), preferentially exhibited death with apoptotic characteristics, with an increase in early apoptotic cells, evident at concentrations as low as 0.2 mM (Fig. 8). Typical nuclear morphology changes of cells undergoing apoptosis, such as condensation and fragmentation of nuclei chromatin, were observed in cells exposed to MDPV at lower concentrations, while necrotic events were only evident at the highest concentrations (0.8 and 1.6 mM). This result is indicative of a bimodal cell death, with apoptosis at lower concentrations and necrosis at higher concentrations. As previously referred in the LDH data (Fig. 3), the supernatants of hepatocytes exposed to MDPV (0.2–1.6 mM) contained significantly higher amounts of LDH all over the experimental period, indicating a loss of integrity of the plasma membrane. It is important to stress at this point that the LDH release assay does not distinguish between primary necrosis and secondary necrosis as a consequence of apoptotic cell death. Based on our findings, any detected LDH release in cells exposed to low concentrations of MDPV is more likely due to secondary necrosis from late apoptotic cells, as no signs of primary necrosis were observed in cells exposed to lower concentrations of the tested drug. Moreover, decreases in MTT reduction, a marker of mitochondrial dysfunction, under the same experimental conditions, further supports an apoptotic cell death mechanism.

Additionally, our data on caspase activity, under normothermic conditions, is in agreement with the induction of apoptosis, though only statistically significant at the highest concentration of MDPV tested. After a 48 h period of incubation, MDPV was able to induce both intrinsic (caspase 9) and extrinsic (caspase 8) apoptotic pathways in primary cultures of rat hepatocytes, which was accompanied by a significant activation of the end-line effector caspase common to both pathways, caspase 3. The occurrence of apoptotic events in the liver was also demonstrated in rats administered with MDMA (Cerretani et al. 2011) and recently described in neonatal mouse brain following MDPV administration (Adam et al. 2014).

Hyperthermia is a toxicological effect that has been associated with the abuse of different cathinone derivatives, particularly MDPV (Borek and Holstege 2012; Kesha et al. 2013; Penders et al. 2012). Although it was already demonstrated that hyperthermia potentiates the toxicity induced by amphetamines in several study models including primary hepatocytes (Carvalho et al. 1997, 2001; Pontes et al. 2008), neuronal cells (Capela et al. 2006) and skeletal muscle (Duarte et al. 1999), it remained unknown whether hyperthermia also increases hepatotoxic responses of the bk-amphetamines analogues. The present study provides irrefutable evidence of the potentiation of MDPV toxicity by hyperthermia as a dramatic decrease in cell viability (Figs. 2, 3), as well as an intensification of all tested oxidative stress endpoints were observed in cells exposed to the drug at 40.5 °C. Hyperthermic conditions heightened MDPV-induced depletion of GSH and formation of ROS and RNS (Figs. 4a, 5, respectively). It is worth to note that the observed potentiation of MDPV-induced GSH depletion by hyperthermia was not due to an increase of GSSG formation. There is compelling evidence in the literature that hyperthermia, *per se*, stimulates a pro-oxidant state in the liver, with the depletion of GSH as a probable initiating event (Skibba et al. 1989, 1991). In accordance, our data showed a decline of intracellular GSH levels in control hepatocytes at 40.5 °C (Fig. 4a), as well as a significant rise in GSSG levels (Fig. 4b). This loss of antioxidant defenses may be in the origin of the intensification of MDPV toxic effects under hyperthermia. The rise in temperature also increased mitochondrial energetic impairment in cells exposed to high MDPV concentrations, leading to a nearly complete ATP depletion (Fig. 6), followed by increased intracellular calcium concentrations (Fig. 7).

Moreover, our data suggest that the increment of 3.5 °C increased cell vulnerability toward necrosis, which advocates a change in the mode of cell death, with the increase in temperature, from apoptosis at physiological temperature, to necrosis under hyperthermic conditions. These findings are in agreement with the ATP levels found in cells. In fact, since apoptosis is an energy-consuming process,

requiring sufficient ATP to occur, the profound ATP depletion attained in cells treated with MDPV (0.4–1.6 mM) at 40.5 °C forces the cell death mechanisms to shift from apoptosis to necrosis. Our results show that hyperthermia hastened activation of apoptotic cell death in MDPV-exposed cells, as evidenced by caspase activation at lower concentrations (Fig. 9), as well as triggered primary necrotic cell death in rat hepatocytes (Fig. 8). These data are corroborated by the observed decline in caspase activity in cells exposed to 1.6 mM MDPV at 40.5 °C, at a concentration where ATP levels are virtually nonexistent and necrosis ensues. The favouring of a necrotic cell death mechanism over apoptosis under hyperthermic conditions was also described in primary cultured rat hepatocytes (Pontes et al. 2008) and HepG2 cells exposed to MDMA (da Silva et al. 2013). Considering that the higher temperature used in our experiment (40.5 °C) matches the body temperatures that recreational abusers may attain after MDPV consumption (Borek and Holstege 2012; Fröhlich et al. 2011; Kesha et al. 2013; Mugele et al. 2012; Murray et al. 2012), our results suggests that MDPV-induced thermoregulation impairment most certainly contributes to increased liver damage.

Finally, it could be argued that the observed hepatotoxic effects occur at relatively high concentrations of the tested drug when compared to the low micromolar concentrations commonly found in MDPV users or in blood of fatal intoxication victims (Kesha et al. 2013; Marinetti and Antonides 2013; Murray et al. 2012; Wyman et al. 2013). However, similar to other drugs like MDMA, whose levels were found to be up to 18 times higher in the liver (De Letter et al. 2006; Garcia-Repetto et al. 2003), the drug concentrations to which hepatocytes are actually exposed may be much higher than those found in blood. Moreover, it must be noted that we used the same concentration range typically used in *in vitro* toxicity studies with amphetamine-type drugs (Beitia et al. 1999; Capela et al. 2006; Carvalho et al. 2004; da Silva et al. 2014; Downey et al. 2014; Pontes et al. 2008). The results from these experiments should be viewed as a way of gaining a better understanding of mechanisms that may be involved in the *in vivo* effects of MDPV.

## Concluding remarks

The data presented in this study strongly suggest that MDPV toxicity in primary cultured rat hepatocytes is mediated by oxidative stress, subsequent to marked GSH depletion, followed by a triangle of events that includes increased ROS and RNS accumulation, mitochondrial dysfunction and perturbation of intracellular Ca<sup>2+</sup> homeostasis, ultimately leading to apoptotic (for lower concentrations)

and necrotic (for higher concentrations) cell death. Both intrinsic (caspase 9 activation) and extrinsic (caspase 8 activation) apoptotic pathways are stimulated, with subsequent activation of the common effector caspase 3. Furthermore, our results clearly indicate that hyperthermia boosts the oxidative stress induced by MDPV in primary rat hepatocytes that ultimately leads to extensive cell death mainly by necrosis. These results suggest that the rise in body temperature after MDPV intake most certainly contributes to the hepatotoxicity that has been reported in humans. Also of great importance, we evidenced the similarities between the toxic events elicited by the MDPV and amphetamines such as MDMA, thus suggesting a correspondence in the mechanism of toxicity of these drugs.

**Acknowledgments** M.J.V. thanks Fundação para a Ciência e Tecnologia (FCT), Portugal, for her PhD Grant (SFRH/BD/89879/2012). This work was supported by FCT, through the Project Pest-C/EQB/LA0006/2013.

## References

- Aarde SM, Huang PK, Creehan KM, Dickerson TJ, Taffe MA (2013) The novel recreational drug 3,4-methylenedioxypyrovalerone (MDPV) is a potent psychomotor stimulant: self-administration and locomotor activity in rats. *Neuropharmacology* 71:130–140. doi:10.1016/j.neuropharm.2013.04.003
- Adam A, Gerecsei LI, Lepesi N, Csillag A (2014) Apoptotic effects of the ‘designer drug’ methylenedioxypyrovalerone (MDPV) on the neonatal mouse brain. *Neurotoxicology* 44:231–236. doi:10.1016/j.neuro.2014.07.004
- Andreu V, Mas A, Bruguera M et al (1998) Ecstasy: a common cause of severe acute hepatotoxicity. *J Hepatol* 29(3):394–397
- Araujo AM, Valente MJ, Carvalho M et al (2015) Raising awareness of new psychoactive substances: chemical analysis and in vitro toxicity screening of ‘legal high’ packages containing synthetic cathinones. *Arch Toxicol*. doi:10.1007/s00204-014-1278-7
- Barbosa DJ, Capela JP, Silva R et al (2014) The mixture of “ecstasy” and its metabolites is toxic to human SH-SY5Y differentiated cells at in vivo relevant concentrations. *Arch Toxicol* 88(2):455–473. doi:10.1007/s00204-013-1120-7
- Baumgartner HK, Gerasimenko JV, Thorne C et al (2009) Calcium elevation in mitochondria is the main Ca<sup>2+</sup> requirement for mitochondrial permeability transition pore (mPTP) opening. *J Biol Chem* 284(31):20796–20803. doi:10.1074/jbc.M109.025353
- Beitia G, Cobreros A, Sainz L, Cenarruzabeitia E (1999) 3,4-Methylenedioxymethamphetamine (ecstasy)-induced hepatotoxicity: effect on cytosolic calcium signals in isolated hepatocytes. *Liver* 19(3):234–241
- Beitia G, Cobreros A, Sainz L, Cenarruzabeitia E (2000) Ecstasy-induced toxicity in rat liver. *Liver* 20(1):8–15
- Borek HA, Holstege CP (2012) Hyperthermia and multiorgan failure after abuse of “bath salts” containing 3,4-methylenedioxypyrovalerone. *Ann Emerg Med* 60(1):103–105. doi:10.1016/j.annemergmed.2012.01.005
- Brookes PS, Yoon Y, Robotham JL, Anders MW, Sheu SS (2004) Calcium, ATP, and ROS: a mitochondrial love-hate triangle. *Am J Physiol Cell Physiol* 287(4):C817–C833. doi:10.1152/ajpcell.00139.2004
- Capela JP, Ruscher K, Lautenschlager M et al (2006) Ecstasy-induced cell death in cortical neuronal cultures is serotonin 2A-receptor-dependent and potentiated under hyperthermia. *Neuroscience* 139(3):1069–1081. doi:10.1016/j.neuroscience.2006.01.007
- Capela JP, Macedo C, Branco PS et al (2007) Neurotoxicity mechanisms of thioether ecstasy metabolites. *Neuroscience* 146(4):1743–1757. doi:10.1016/j.neuroscience.2007.03.028
- Carhart-Harris RL, King LA, Nutt DJ (2011) A web-based survey on mephedrone. *Drug Alcohol Depend* 118(1):19–22. doi:10.1016/j.drugalcdep.2011.02.011
- Carvalho F, Remião F, Soares ME, Catarino R, Queiroz G, Bastos ML (1997) d-Amphetamine-induced hepatotoxicity: possible contribution of catecholamines and hyperthermia to the effect studied in isolated rat hepatocytes. *Arch Toxicol* 71(7):429–436
- Carvalho M, Carvalho F, Bastos ML (2001) Is hyperthermia the triggering factor for hepatotoxicity induced by 3,4-methylenedioxymethamphetamine (ecstasy)? An in vitro study using freshly isolated mouse hepatocytes. *Arch Toxicol* 74(12):789–793
- Carvalho M, Milhazes N, Remiao F et al (2004) Hepatotoxicity of 3,4-methylenedioxymethamphetamine and alpha-methyl dopamine in isolated rat hepatocytes: formation of glutathione conjugates. *Arch Toxicol* 78(1):16–24. doi:10.1007/s00204-003-0510-7
- Carvalho M, Pontes H, Remiao F, Bastos ML, Carvalho F (2010) Mechanisms underlying the hepatotoxic effects of ecstasy. *Curr Pharm Biotechnol* 11(5):476–495
- Carvalho M, Carmo H, Costa VM et al (2012) Toxicity of amphetamines: an update. *Arch Toxicol* 86(8):1167–1231. doi:10.1007/s00204-012-0815-5
- Cerretani D, Bello S, Cantatore S et al (2011) Acute administration of 3,4-methylenedioxymethamphetamine (MDMA) induces oxidative stress, lipoperoxidation and TNF $\alpha$ -mediated apoptosis in rat liver. *Pharmacol Res* 64(5):517–527. doi:10.1016/j.phrs.2011.08.002
- Coppola M, Mondola R (2012a) 3,4-methylenedioxypyrovalerone (MDPV): chemistry, pharmacology and toxicology of a new designer drug of abuse marketed online. *Toxicol Lett* 208(1):12–15. doi:10.1016/j.toxlet.2011.10.002
- Coppola M, Mondola R (2012b) Synthetic cathinones: chemistry, pharmacology and toxicology of a new class of designer drugs of abuse marketed as “bath salts” or “plant food”. *Toxicol Lett* 211(2):144–149. doi:10.1016/j.toxlet.2012.03.009
- De Letter EA, Piette MH, Lambert WE, Cordonnier JA (2006) Amphetamines as potential inducers of fatalities: a review in the district of Ghent from 1976–2004. *Med Sci Law* 46(1):37–65
- Deluca P, Schifano F, Davey Z, Corazza O, Di Furia L, Group PWMR (2009) MDPV report. <http://www.psychonautproject.eu/>
- den Hollander B, Sundstrom M, Pelander A et al (2014) Keto amphetamine toxicity-focus on the redox reactivity of the cathinone designer drug mephedrone. *Toxicol Sci* 141(1):120–131. doi:10.1093/toxsci/kfu108
- da Silva DD, Carmo H, Lynch A, Silva E (2013) An insight into the hepatocellular death induced by amphetamines, individually and in combination: the involvement of necrosis and apoptosis. *Arch Toxicol* 87(12):2165–2185. doi:10.1007/s00204-013-1082-9
- da Silva DD, Silva E, Carmo H (2014) Combination effects of amphetamines under hyperthermia—the role played by oxidative stress. *J Appl Toxicol* 34(6):637–650. doi:10.1002/jat.2889
- Downey C, Daly F, O’Boyle KM (2014) An in vitro approach to assessing a potential drug interaction between MDMA (ecstasy) and caffeine. *Toxicol In Vitro* 28(2):231–239. doi:10.1016/j.tiv.2013.10.021
- Duarte JA, Carvalho F, Natsis K et al (1999) Structural alterations of skeletal muscle induced by chronic administration of Damphetamine and food restriction. *Basic Appl Myol* 9(2):65–69
- EMCDDA (2015) New psychoactive substances in Europe. An update from the EU Early Warning System. Euro surveillance:

- bulletin European sur les maladies transmissibles = European communicable disease bulletin. <http://www.emcdda.europa.eu/>. doi:10.2810/372415
- EMCDDA-Europol (2014) EMCDDA—Europol Joint Report on a new psychoactive substance: MDPV (3,4-methylenedioxypropylvalerone). <http://www.emcdda.europa.eu/>. doi:10.2810/24085
- Fantegrossi WE, Gannon BM, Zimmerman SM, Rice KC (2013) In vivo effects of abused ‘bath salt’ constituent 3,4-methylenedioxypropylvalerone (MDPV) in mice: drug discrimination, thermoregulation, and locomotor activity. *Neuropsychopharmacology* 38(4):563–573. doi:10.1038/npp.2012.233
- Fröhlich S, Lambe E, O’Dea J (2011) Acute liver failure following recreational use of psychotropic “head shop” compounds. *Ir J Med Sci* 180(1):263–264. doi:10.1007/s11845-010-0636-6
- Garcia-Repetto R, Moreno E, Soriano T, Jurado C, Gimenez M, Menendez M (2003) Tissue concentrations of MDMA and its metabolite MDA in three fatal cases of overdose. *Forensic Sci Int* 135(2):110–114
- Gatch MB, Taylor CM, Forster MJ (2013) Locomotor stimulant and discriminative stimulus effects of ‘bath salt’ cathinones. *Behav Pharmacol* 24(5–6):437–447. doi:10.1097/FBP.0b013e328364166d
- German CL, Fleckenstein AE, Hanson GR (2014) Bath salts and synthetic cathinones: an emerging designer drug phenomenon. *Life Sci* 97(1):2–8. doi:10.1016/j.lfs.2013.07.023
- Halestrap AP (2006) Calcium, mitochondria and reperfusion injury: a pore way to die. *Biochem Soc Trans* 34(Pt 2):232–237. doi:10.1042/BST20060232
- Halestrap AP (2009) What is the mitochondrial permeability transition pore? *J Mol Cell Cardiol* 46(6):821–831. doi:10.1016/j.yjmcc.2009.02.021
- James D, Adams RD, Spears R et al (2011) Clinical characteristics of mephedrone toxicity reported to the UK National Poisons Information Service. *Emerg Med J* 28(8):686–689. doi:10.1136/emj.2010.096636
- Johnson PS, Johnson MW (2014) Investigation of “bath salts” use patterns within an online sample of users in the United States. *J Psychoact Drugs* 46(5):369–378. doi:10.1080/02791072.2014.962717
- Jones S, Fileccia EL, Murphy M et al (2014) Cathinone increases body temperature, enhances locomotor activity, and induces striatal c-fos expression in the Siberian hamster. *Neurosci Lett* 559:34–38. doi:10.1016/j.neulet.2013.11.032
- Kamijo Y, Soma K, Nishida M, Namera A, Ohwada T (2002) Acute liver failure following intravenous methamphetamine. *Vet Hum Toxicol* 44(4):216–217
- Kanel GC, Cassidy W, Shuster L, Reynolds TB (1990) Cocaine-induced liver cell injury: comparison of morphological features in man and in experimental models. *Hepatology* 11(4):646–651
- Kesha K, Boggs CL, Ripple MG et al (2013) Methylenedioxypropylvalerone (“bath salts”), related death: case report and review of the literature. *J Forensic Sci* 58(6):1654–1659. doi:10.1111/1556-4029.12202
- Leier I, Jedlitschky G, Buchholz U et al (1996) ATP-dependent glutathione disulphide transport mediated by the MRP gene-encoded conjugate export pump. *Biochem J* 314(Pt 2):433–437
- Lopez-Arnau R, Martinez-Clemente J, Pubill D, Escubedo E, Camarasa J (2012) Comparative neuropharmacology of three psychostimulant cathinone derivatives: butylone, mephedrone and methylone. *Br J Pharmacol* 167(2):407–420. doi:10.1111/j.1476-5381.2012.01998.x
- Lopez-Arnau R, Martinez-Clemente J, Rodrigo T, Pubill D, Camarasa J, Escubedo E (2015) Neuronal changes and oxidative stress in adolescent rats after repeated exposure to mephedrone. *Toxicol Appl Pharmacol*. doi:10.1016/j.taap.2015.03.015
- Marinetti LJ, Antonides HM (2013) Analysis of synthetic cathinones commonly found in bath salts in human performance and postmortem toxicology: method development, drug distribution and interpretation of results. *J Anal Toxicol* 37(3):135–146. doi:10.1093/jat/bks136
- McIlwain DR, Berger T, Mak TW (2013) Caspase functions in cell death and disease. *Cold Spring Harb Perspect Biol* 5(4):a008656. doi:10.1101/cshperspect.a008656
- Meyer MR, Du P, Schuster F, Maurer HH (2010) Studies on the metabolism of the alpha-pyrrolidinophenone designer drug methylenedioxy-propylvalerone (MDPV) in rat and human urine and human liver microsomes using GC–MS and LC–high-resolution MS and its detectability in urine by GC–MS. *J Mass Spectrom* 45(12):1426–1442. doi:10.1002/jms.1859
- Meyer MR, Richter LH, Maurer HH (2014) Methylenedioxy designer drugs: mass spectrometric characterization of their glutathione conjugates by means of liquid chromatography-high-resolution mass spectrometry/mass spectrometry and studies on their glutathionyl transferase inhibition potency. *Anal Chim Acta* 822:37–50. doi:10.1016/j.aca.2014.03.017
- Miller ML, Creehan KM, Angrish D et al (2013) Changes in ambient temperature differentially alter the thermoregulatory, cardiac and locomotor stimulant effects of 4-methylmethcathinone (mephedrone). *Drug Alcohol Depend* 127(1–3):248–253. doi:10.1016/j.drugalcdep.2012.07.003
- Mugele J, Nanagas KA, Tormoehlen LM (2012) Serotonin syndrome associated with MDPV use: a case report. *Ann Emerg Med* 60(1):100–102. doi:10.1016/j.annemergmed.2011.11.033
- Murray BL, Murphy CM, Beuhler MC (2012) Death following recreational use of designer drug “bath salts” containing 3,4-methylenedioxypropylvalerone (MDPV). *J Med Toxicol* 8(1):69–75. doi:10.1007/s13181-011-0196-9
- Penders TM, Gestring RE, Vilensky DA (2012) Excited delirium following use of synthetic cathinones (bath salts). *Gen Hosp Psychiatry* 34(6):647–650. doi:10.1016/j.genhosppsych.2012.06.005
- Pontes H, Sousa C, Silva R et al (2008) Synergistic toxicity of ethanol and MDMA towards primary cultured rat hepatocytes. *Toxicology* 254(1–2):42–50. doi:10.1016/j.tox.2008.09.009
- Shortall SE, Green AR, Swift KM, Fone KC, King MV (2013) Differential effects of cathinone compounds and MDMA on body temperature in the rat, and pharmacological characterization of mephedrone-induced hypothermia. *Br J Pharmacol* 168(4):966–977. doi:10.1111/j.1476-5381.2012.02236.x
- Skibba JL, Stadnicka A, Kalbfleisch JH, Powers RH (1989) Effects of hyperthermia on xanthine oxidase activity and glutathione levels in the perfused rat liver. *J Biochem Toxicol* 4(2):119–125
- Skibba JL, Powers RH, Stadnicka A, Cullinane DW, Almagro UA, Kalbfleisch JH (1991) Oxidative stress as a precursor to the irreversible hepatocellular injury caused by hyperthermia. *Int J Hyperther* 7(5):749–761
- Strano-Rossi S, Cadwallader AB, de la Torre X, Botre F (2010) Toxicological determination and in vitro metabolism of the designer drug methylenedioxypropylvalerone (MDPV) by gas chromatography/mass spectrometry and liquid chromatography/quadrupole time-of-flight mass spectrometry. *Rapid Commun Mass Spectrom* 24(18):2706–2714. doi:10.1002/rcm.4692
- Tait SW, Green DR (2010) Mitochondria and cell death: outer membrane permeabilization and beyond. *Nat Rev Mol Cell Biol* 11(9):621–632. doi:10.1038/nrm2952
- Tsujimoto Y (2003) Cell death regulation by the Bcl-2 protein family in the mitochondria. *J Cell Physiol* 195(2):158–167. doi:10.1002/jcp.10254
- Valente MJ, Henrique R, Vilas-Boas V et al (2012) Cocaine-induced kidney toxicity: an in vitro study using primary cultured human proximal tubular epithelial cells. *Arch Toxicol* 86(2):249–261. doi:10.1007/s00204-011-0749-3

- Valente MJ, Guedes de Pinho P, de Lourdes Bastos M, Carvalho F, Carvalho M (2014) Khat and synthetic cathinones: a review. *Arch Toxicol* 88(1):15–45. doi:[10.1007/s00204-013-1163-9](https://doi.org/10.1007/s00204-013-1163-9)
- Varner KJ, Daigle K, Weed PF et al (2013) Comparison of the behavioral and cardiovascular effects of mephedrone with other drugs of abuse in rats. *Psychopharmacology* 225(3):675–685. doi:[10.1007/s00213-012-2855-1](https://doi.org/10.1007/s00213-012-2855-1)
- Wills EJ, Findlay JM, McManus JP (1976) Effects of hyperthermia therapy on the liver. II. Morphological observations. *J Clin Pathol* 29(1):1–10
- Wood DM, Davies S, Greene SL et al (2010) Case series of individuals with analytically confirmed acute mephedrone toxicity. *Clin Toxicol* 48(9):924–927. doi:[10.3109/15563650.2010.531021](https://doi.org/10.3109/15563650.2010.531021)
- Wyman JF, Lavins ES, Engelhart D et al (2013) Postmortem tissue distribution of MDPV following lethal intoxication by “bath salts”. *J Anal Toxicol* 37(3):182–185. doi:[10.1093/jat/bkt001](https://doi.org/10.1093/jat/bkt001)
- Zuba D, Byrska B (2013) Prevalence and co-existence of active components of ‘legal highs’. *Drug Test Anal* 5(6):420–429. doi:[10.1002/dta.1365](https://doi.org/10.1002/dta.1365)